THE EFFECTS OF THE INSTALLATION LOCATION OF PROPULSIVE ROTOR ON THE AERODYNAMIC CHARACTERISTICS FOR ABC HELICOPTERS

Wei-Liang Lyu
State Key Laboratory of Structural Analysis for Industrial Equipment
Dalian University of Technology, Dalian 116024,
P. R. China

Guo-Hua Xu
National Key Laboratory of Rotorcraft Aeromechanics
Nanjing University of Aeronautics and Astronautics, Nanjing 210016
P. R. China

Abstract

Based on the free-wake method, a comprehensive model for the analysis of the aerodynamic characteristics of ABC rotor propeller-augmented compound helicopters is established and a new trim method for the multi-control solutions of ABC helicopters is presented. The developed model is utilized to investigate the aerodynamic interference characteristics of the main rotors on the propulsive rotor and the effects of the installation location of propulsive rotor on its aerodynamic characteristics. Numerical examples show that in certain range of forward flying speed, the aerodynamic interference characteristics of the blades of main rotors on the front propulsive rotor will improve the aerodynamic performance, decrease the power consumption and decrease the vibration level of thrust of the front propulsive rotor. This advantage will be weakened, if the vertical spacing between the propeller hub of the propulsive rotor and the lower main rotor disc is increased too much. On the other hand, however, the direct aerodynamic impacts of the wake of main rotors on the regular rear propulsive rotor will degrade the aerodynamic performance, increase the power consumption and increase the vibration level of thrust of the regular rear propulsive rotor.

1. INTRODUCTION

Helicopters have lower cruise speed than fixed-wing aircrafts. Research on new configurations of high-speed helicopters have been conducted to overcome this disadvantage. The Advancing Blade Concept (ABC) rotor[1] propeller-augmented compound helicopter[2,3] (also called ABC helicopter) is one of the most successful configurations; the X-2 helicopter is a representative of such configurations. The X-2 helicopter maintains and develops the technical features of conventional helicopters[1], which is an important direction for the development of future helicopters. However, the special configuration of this helicopter causes complicated interactional aerodynamics.

The common configuration of the ABC helicopter includes coaxial main rotors with a propeller rotor[4]. Many theoretical and experimental investigations have been performed for conventional coaxial helicopters; vortex theory[5,6] and CFD method[7,8] are often employed as theoretical analytical tools. The interactional aerodynamics of an ABC helicopter changes significantly when a propeller rotor is compounded into a conventional coaxial helicopter. Previous analytical tools cannot be directly applied to the new configuration. Meanwhile, theoretical studies on ABC rotor propeller-augmented compound helicopters, particularly helicopters capable of analyzing the interactional aerodynamic characteristics of the main aerodynamic components, are rare in current publication.

In 2008, Kim et al.[9] built the first comprehensive model for analyzing the interactional aerodynamics of ABC helicopters. In their model, VTM method[10], which is a viscous vortex method, was used. Kim et al. comprehensively analyzed the aerodynamic characteristics of the main rotors, horizontal tail plane, and propeller rotor at different forward-flight conditions. However, numerous computations[11] had to be performed because of VTM method's application; this condition resulted in the establishment of a simplified helicopter trim model[12]. In the simplified trim model, similar cyclic pitch controls were inputted to the upper and lower main rotors [9,13,14].

Trim analysis is important for aerodynamic calculations of the ABC helicopter. According to Burgess[1], the lateral lift offset control of the main rotors is the essence of the ABC concept. This condition means that for an ABC rotor propeller-augmented compound helicopter, multi-trimmed control solutions exist at each flight condition; performance optimization, rotor moments, and vibration are readily affected by the use of differential cyclic and collective pitch. This control technique has a significant research value[15,16]. The technique cannot be implemented by applying a simplified trim method with a single-control solution for each flight condition. Therefore, the setup of a trim model that can obtain multi-control solutions for each flight condition is significant but challenging.

On the other hand, the propulsive rotor is an key part for the ABC helicopter. At high forward speed, compressibility at the tip of the advancing blade will weaken the aerodynamic performance of the rotor regardless of the flapwise stiffness of the system. And the effects of compressibility can be delayed to higher forward speed however if the main rotor system can be off-loaded by a suitable means of lift or thrust augmentation, thus allowing for reduced rotational speed of the main rotor[3]. At first, a pair of turbojets or a turbofan was selected to augment the thrust produced by the main rotor. However, the turbojet and the turbofan were almost abandoned for the compound helicopter because of its inefficiency and noise. They will also result in a power redundancy on the aircraft as the power from them cannot be used during hovering flight. From this point of view, the propeller will be a more appropriate choice to off-load the main rotors for an ABC helicopter.

However, this kind of thrust-augmented device, although being crucial for the ABC helicopter to increase the forward flying speed, but will cause another complicated situation to the aerodynamic characteristics of an ABC helicopter. For a regular rear-installed propulsive rotor, it will be strongly affected by the wake of main rotors under certain flight conditions. Just as pointed out by Orchard and Newman[3], The interactions between the rotor wake and propeller present an unknown factor, although effects similar to the tail rotor-main rotor wake blade vortex interaction effect must be expected, but only for certain portions of the flight envelope. In order to maximise the efficiency and potential of this type of aircraft, a thorough understanding of the nature and form of the aerodynamic interactions that occur within the system, as well as an appreciation of the flight conditions under which such interactions might pose the greatest challenges to the operation and control of the vehicle, is essential.

From this point of view, in this research, based on the free-wake method, a comprehensive calculation model of an ABC rotor propeller-augmented compound helicopter will be established to investigate its interactional aerodynamic characteristics. And a new trim method for multi control solutions is presented. This research is focusing on the aerodynamic interference characteristics of the main rotors on the propulsive rotor and the effects of the installation location of propulsive rotor on its aerodynamic characteristics. And some new conclusions will be drawn.

2. MODEL AND METHODOLOGY

2.1 Computational Model

Because of the lack of detailed data in publication of the main rotors of X-2 high-speed helicopter, the calculation model of ABC-rotor propeller-augmented compound helicopter applied in this paper is partially simplified from the data of XH-59A and X-2 helicopters in order to fit the free-wake method. The calculation model is schematically shown in Fig. 1.

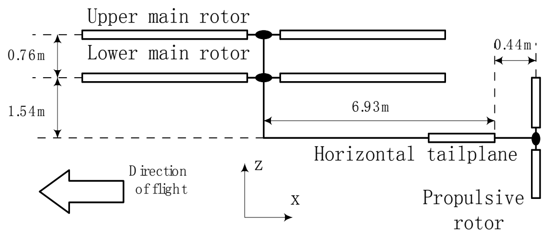

Fig. 1 Schematic of the configuration of ABC rotor propeller-augmented compound helicopters

As shown in Fig. 1, configuration of the calculation model is similar to X-2, i.e. a generic helicopter configuration that comprises a stiffened twin coaxial rotor system together with an auxiliary tail propeller and a horizontal tailplane. The horizontal tailplane is untwisted and has a rectangular planform (3.74m*0.94m). Its airfoil section is NACA0012.

The main rotor system modeled in this study contains two counter-rotating three-bladed rotors, which are separated axially. The blades of both rotors are tapered linearly in planform and have -10° of linear twist and 5.5m of rotor radius. The twin rotors of the coaxial system are arranged so that the lower rotor rotates anticlockwise and the upper one rotates clockwise when viewed from above. The rotors have been arranged to overlap when blades from both the upper and the lower rotors pass directly over the centreline of the rear fuselage. For simplicity, a constant airfoil section, NACA0012, is used along the entire span of the rotor blades.

The geometric properties of the main rotor system are summarized in Table 1.

Table 1 Main rotor and propulsive rotor geometries

	Main rotor	propulsor
Rotor radius (m)	5.5	1.54
Number of rotors	2	1
Blades per rotor	3	5
Root cutout	0.12	0.2
Twist (°)	-10	-30
Tip Chord (m)	0.554	0.2772
Taper	2	1
Airfoil sections	NACA0012	NACA0012

In addition, a five-bladed propeller is used to represent an auxiliary thrust-producing device mounted in pusher configuration to the rear of the fuselage. The blades of this propulsive rotor feature a tapered root end, -30° of linear twist, and a NACA0012 sectional profile. Its rotational speed is fixed at 4 times the main rotor speed and its direction of rotation is anticlockwise when seen from the rear of the aircraft. A summary of the geometry of the propulsive rotor is given in Table 1.

2.2 Free-wake Method

In this paper, the rotor wake is calculated by the time-marching free-wake method[17], which divides the wake filament into lots of straight vortex segments. Each segment moves with the local velocity, whose governing equation can be given as

$$\frac{\mathrm{d}\boldsymbol{r}}{\mathrm{dt}} = \boldsymbol{v}(\boldsymbol{r},\mathrm{t}) \tag{1}$$

where $\boldsymbol{r}$ represents the position vector of the vortex node, and $\boldsymbol{v}$ is the local velocity.

To any node along the rotor wake filament, the 4th-order accurate Adams-Bashforth-Moulton predictor-corrector scheme[18] is applied, which is

$$\begin{aligned}&\textbf{\textit{Predictor}}\text{:}\ \boldsymbol{r}^*_{t+4\Delta t} = \boldsymbol{r}_{t+3\Delta t} + \\ &\frac{h}{24}\left(55\boldsymbol{v}_{t+3\Delta t} - 59\boldsymbol{v}_{t+2\Delta t} + 37\boldsymbol{v}_{t+\Delta t} - 9\boldsymbol{v}_t\right) \\ &\textbf{\textit{Corrector}}\text{:}\ \boldsymbol{r}_{t+4\Delta t} = \boldsymbol{r}_{t+3\Delta t} + \\ &\frac{h}{24}\left(9\boldsymbol{v}^*_{t+4\Delta t} + 19\boldsymbol{v}_{t+3\Delta t} - 5\boldsymbol{v}_{t+2\Delta t} + \boldsymbol{v}_{t+\Delta t}\right)\end{aligned} \tag{2}$$

where the predictor of the explicit 4th-order accurate Adams-Bashforth method will firstly give a predicted solution $\boldsymbol{r}^*_{t+4\Delta t}$, then the corrector of the implicit one will obtain the final solution $\boldsymbol{r}_{t+4\Delta t}$. The verification of the reliability of this predictor-corrector scheme can be found in other references, which therefore will not be given here again.

2.3 Trim Methodology

During the flight of a helicopter, pilots change the flight condition and the aerodynamic force by controlling the rotor inputs. Therefore, to obtain the accurate control data, a proper trim model should be contained in the analysis of interactional aerodynamic characteristics of a helicopter. As mentioned before, within the few studies of interactional aerodynamic characteristics of ABC helicopters, because of the huge amount of computations, a simplified helicopter trim model was carried out in their method. In their simplified trim model, same cyclic pitch control was inputted to both the upper and the lower main rotors[9].

On the other hand, in the current study, a more complicated trim methodology is presented instead of the former simplified one.

Specifically， different from the trim model of an isolated rotor, for an ABC helicopter, there are more control input quantities. Seven important ones of them are picked up, which are the collective pitch and cyclic pitch of the lower rotor, $A0_L$, $A1_L$ and $A2_L$, collective pitch and cyclic pitch of the upper rotor, $A0_U$, $A1_U$ and $A2_U$, collective pitch of propulsive rotor, $A0_P$. Then the control input vector of an ABC helicopter can be given as

$$\boldsymbol{z} = \left(A0_L, A1_L, A2_L, A0_U, A1_U, A2_U, A0_P\right)^T \tag{3}$$

Where the blade pitch of main rotors can be defined by azimuth angle ψ as

$$\begin{aligned}&\theta_i(\psi) = A0_i + A1_i \cdot \cos(\psi) + A2_i \cdot \sin(\psi) \\ &, i = L,U\end{aligned} \tag{4}$$

As shown in Fig. 1, the xyz-coordinate system is adopted. The Cartesian components of the overall forces and moments constitute the trim state vector, i.e.

$$\boldsymbol{y} = \left(F_x, F_y, F_z, M_x, M_y, M_z\right)^T \tag{5}$$

In order to match the number of control input variables with that of the trim ones, the lateral force, F_y, will be ignored, which is much weaker than the other forces. And the cyclic pitch inputs of the upper rotor, $A1_U$ and $A2_U$, will be used as the default values, which do not change during the trim process. In such way, failure of solving trim equation could be avoided. Therefore, both the control input and the trim state quantity consist of 5 components. They can be regiven as follows

$$\bar{\boldsymbol{z}} = \left(A0_L, A1_L, A2_L, A0_U, A0_P\right)^T \tag{6}$$

$$\bar{\boldsymbol{y}} = \left(F_x, F_z, M_x, M_y, M_z\right)^T \tag{7}$$

It should be pointed out, the default values, $A1_U$ and $A2_U$, need to be chosen carefully, which means that improper values will lead to the failure of solving the trim equation.

So, the trim equation can be given as

$$\Delta\bar{\boldsymbol{z}} = \lambda \boldsymbol{J}^{-1}\Delta\bar{\boldsymbol{y}} \tag{8}$$

Where $\boldsymbol{J}$ is the Jacobean matrix, and $\lambda\left(0<\lambda\le 1\right)$ is a relaxation factor used to maintain the numerical stability.

To verify the reliability of this trim methodology, the flight condition at advance ratio of 0.15 is chosen as a numerical example. Fig. 2 gives convergence process of the control input and trim variables. As shown in Fig. 2 (a), all the five trim state data have converged from various initial values to zero. On the other hand, as shown in Fig. 2 (b), all the five control input data have converged to some specific values accordingly. It can be seen from this trim procedure that the trim methodology presented in this paper is reliable and effective in finding a trim state under specified flight conditions and getting corresponding control input data. Moreover, different from the conventional simplified trim method, by assigning different default values, $A1_U$ and $A2_U$, present trim methodology can find much more trim states under one specified flight condition to investigate the interactional aerodynamic characteristics of ABC helicopters more deeply.

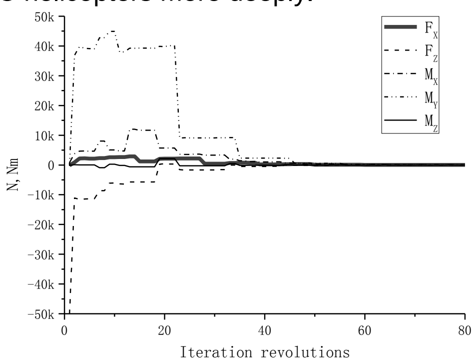

(a) Trim state data

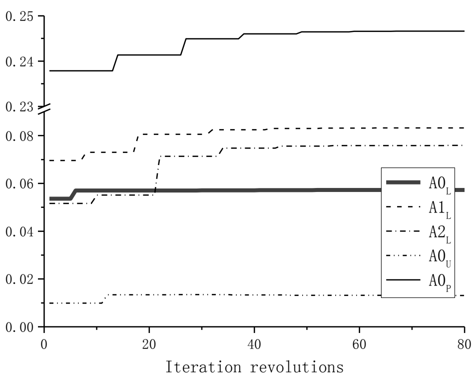

(b) Control input data

Fig. 2 Convergence process of the control input and trim variables (μ=0.15)

3. RESULTS AND ANALYSES

3.1 Thrust Vibration of Propulsor

Figure. 3 presents the temporal variation in propulsor thrust and power over one main rotor revolution, with the helicopter trimed into forward flight at the various advance ratios. As shown in the figure, along with the growth of forward flight speed, the thrust produced by the propulsor is increasing. And the power consumption is accordingly rising. It should be pointed out, there are two types of vibration frequency existing in the temporal variation in propulsor thrust and power over one main rotor revolution at the same time. One strong 3Ω component has a relatively longer wavelength, and another component has a much higher frequency of about 20Ω.

Between these two types of vibration frequency, the strong 3Ω component is mainly caused by the wake of main rotors. On the other hand, the other higher frequency of about 20Ω is coming from the rotation of the propulsive rotor. Because the propulsive rotor has 5 blades, rotating at a frequency four times higher than the one of main rotors. Therefore, when the distribution of blade loading over the propulsive rotor disc is not even, the propulsive rotor will generate a high vibration frequency 20 times higher than the rotating frequency of main rotors, i.e. 20Ω.

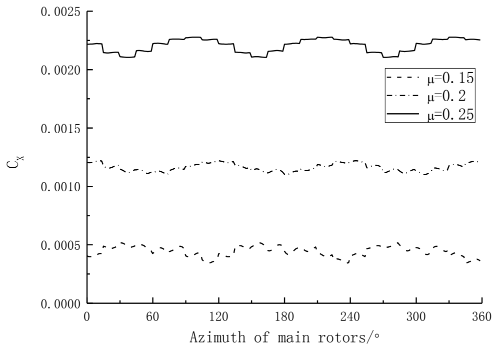

(a) Thrust coefficient

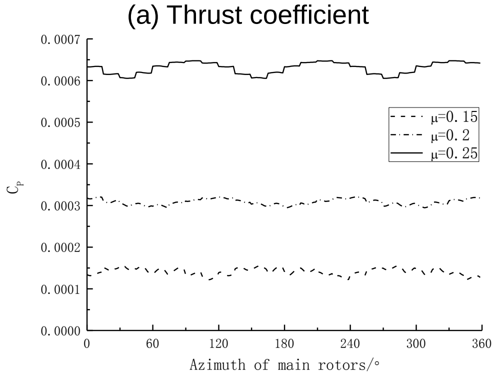

(b) Power coefficient

Fig. 3 Temporal variation in the thrust and power of the propulsive rotor over one revolution of main rotors at various advance ratios

It has to be pointed out, besides the vibration frequency characteristics of the propulsive rotor obtained by the free wake method here, the VTM (Vorticity Transport Model) can get similar results[9]. These two groups of results are not completely identical, because of the different calculating methods, calculating models and trim states being applied by these two researches. But the vibration frequency characteristics of the propulsive rotor being obtained by these two different methods are still very similar, i. e. there are two types of vibration frequency existing in the temporal variation in propulsor thrust and power over one main rotor revolution at the same time, i. e. one strong 3Ω component and one high-frequency 20Ω component. It can be seen, even the vibration frequency characteristics of the propulsive rotor cannot be verified directly by experimental data so far, the similar calculating results of these two methods could verify their validity for each other.

Furthermore, Fig. 4 presents the Distribution of thrust over the propulsive rotor at various advance ratios, where darker area represents higher loading. As shown in the figure, because of the effects of down wash flow of main rotors, the blades of propulsive rotor can be distinguished into two different operation conditions, i.e. the “climbing blade” and the “descending blade”. In the propulsive rotor disc, the “climbing blade” moves against the down wash flow of main rotors, therefore obtaining larger inflow velocity on the airfoil section and generating greater thrust. On the other hand, the “descending blade” moves along with the down wash flow of main rotors, therefore obtaining smaller inflow velocity on the airfoil section and generating less thrust. As shown in Fig. 4, as the propulsive rotor is rotating anticlockwise, a blade on the right side will be a “climbing blade”, and one on the left side should be a “descending blade”. These two different operation conditions of the propulsive rotor are similar to the two different operation conditions of “advancing/retreating blade” of main rotors because of the effects of forward flying speed. It should be noticed, the speed of down wash flow of main rotors is much smaller than the forward flying speed for a helicopter, especially for an ABC helicopter. It makes the difference between “climbing/descending blade” is smaller than the one between “advancing/retreating blade”. Even so, it can be seen from Fig. 4, larger forward flying speed will generate greater down wash flow of main rotors, which will aggravate the difference between “climbing/descending blades”.

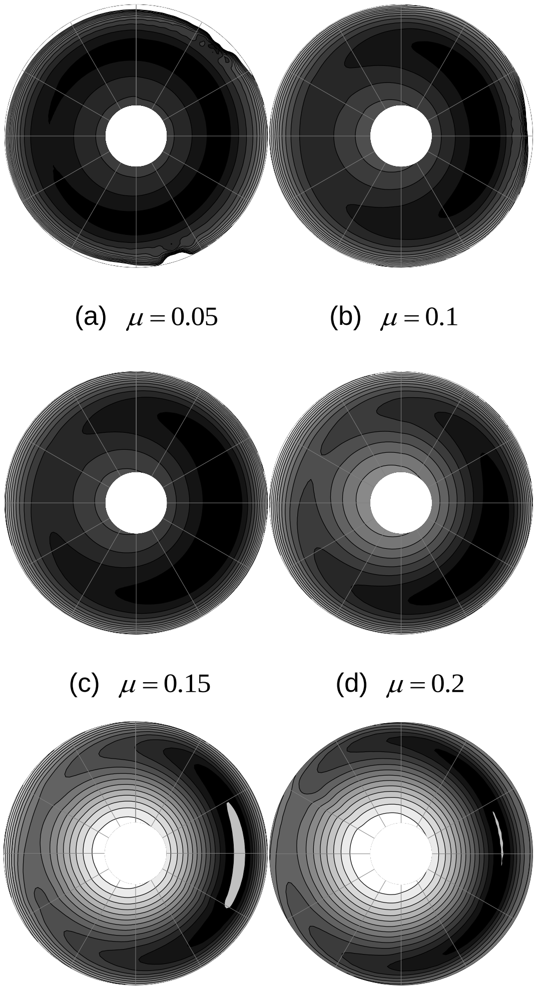

(a) $\mu = 0.05$ (b) $\mu = 0.1$

(c) $\mu = 0.15$ (d) $\mu = 0.2$

(e) $\mu = 0.25$ (f) $\mu = 0.3$

Fig. 4 Distribution of thrust over the propulsive rotor at various advance ratios

Moreover, Fig. 5 shows the distribution of inflow over the propulsive rotor at various advance ratios, where darker area represents larger values. It could be noticed, except the results at the advance ratio of 0.05, showing a distribution characteristic of center-diverging, all the other distributions of inflow over the propulsive rotor are presenting a distribution characteristic of horizontal-banding. This situation could be explained by the side view of wake of main rotors at various advance ratios, given by Fig. 6. As shown in the figure, when the ABC helicopter is flying at a low advance ratio such as 0.05, the wake of main rotors is being down-washed under the propulsive rotor, with no direct aerodynamic interference to the propulsive rotor. On the other hand, at higher advance ratios, the wake of main rotors will directly aerodynamic impact on the propulsive rotor at different levels. As shown in Fig. 6 (b)~(d), with the increasing of forward flying speed, the wake of main rotors is becoming more horizontal and the impacting zone on the propulsive rotor disc is moving further upward. Under this kind of directly aerodynamic impact, distributions of inflow over the propulsive rotor are presenting a distribution characteristic of horizontal-banding, as shown in Fig. 5, and there is greater inflow in the impacted zone. It can also be seen, with the increasing of forward flying speed, the impacted zone is moving further upward, as shown in Fig. 5 (b)~(d), matching the results of Fig. 6. Therefore, it can be seen, the direct aerodynamic impacts of the wake of main rotors on the propulsive rotor could raise the speed of inflow in the impacting zone on the propulsive rotor. These aerodynamic interference characteristics will be further analyzed in the next section.

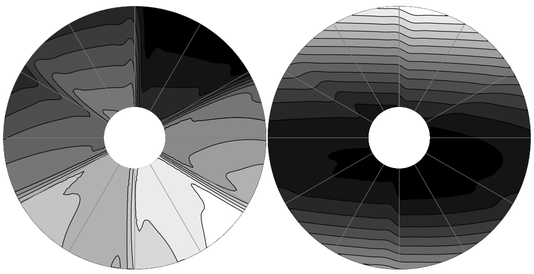

(a) $\mu = 0.05$ (b) $\mu = 0.1$

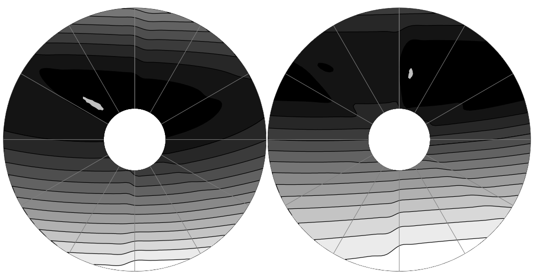

(c) $\mu = 0.15$ (d) $\mu = 0.2$

Fig. 5 Distribution of inflow over the propulsive rotor at various advance ratios

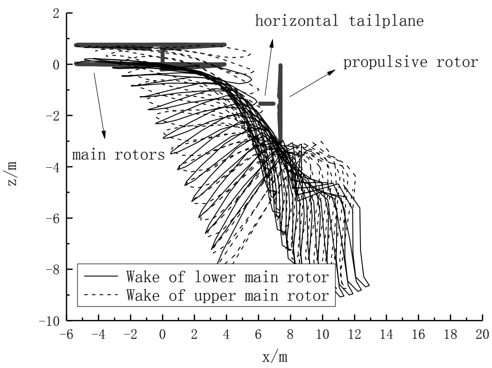

(a) $\mu = 0.05$

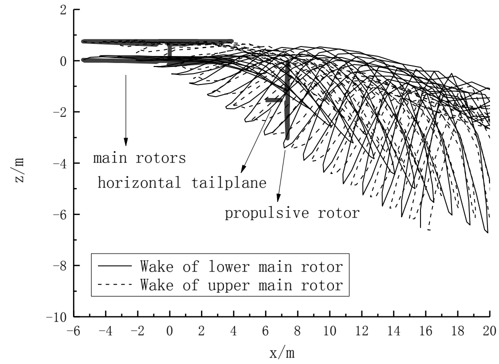

(b) $\mu = 0.1$

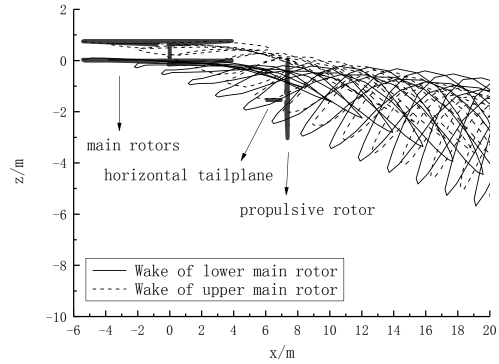

(c) $\mu = 0.15$

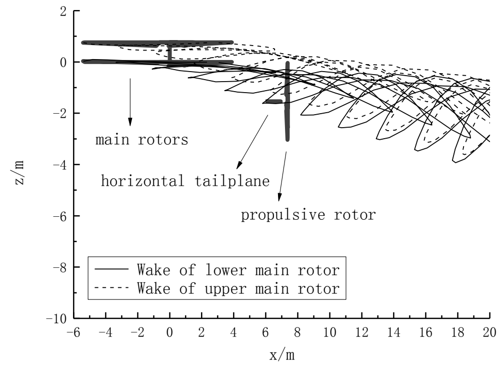

(d) $\mu = 0.2$

Fig. 6 Side view of wake of main rotors at various advance ratios

3.2 Effects of the Installation Location of Propulsive Rotor on the Aerodynamic Characteristics

For some reasons, regular advancing Blade Concept rotor propeller-augmented compound helicopters are rear-propeller-augmented, such as the X2 and S97. However, the wake of main rotors will make direct aerodynamic impacts on the propulsive rotor, as discussed before. Then, in this section, the effects of the installation location of propulsive rotor on the aerodynamic characteristics will be investigated by calculating the aerodynamic interference characteristics of the propeller rotor for an ABC rotor front-propeller-augmented compound helicopter.

And the results will be compared with the ones of a regular rear-propeller-augmented ABC helicopter, in the purpose of providing the reference for the design of the installation location of the propulsive rotor.

Fig. 5 gives the Schematic of the configuration of ABC rotor front-propeller-augmented compound helicopters. As shown in the figure, the propulsive rotor is front-installed. The distance between the shaft of the propulsive rotor and the lower main rotor disc is expressed as gZ. The installation locations of other components are set to be as same as them in Fig. 1.

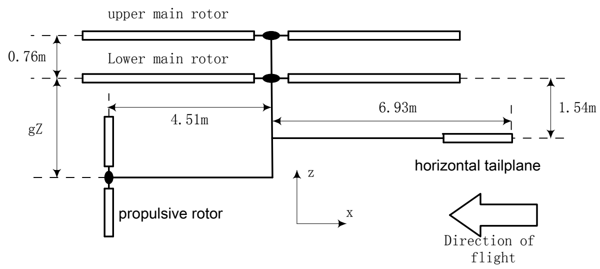

Fig. 7 Schematic of the configuration of ABC rotor front-propeller-augmented compound helicopters

First, set $gZ = 0.56R$, the new helicopter model is retrimed and recalculated. Fig. 8(a) ~ Fig. 11(a) show the temporal variation in the thrust of the rear/front propulsive rotor over one revolution of main rotors at the advance ratio of 0.15, 0.2, 0.25 and 0.3. As shown in these figures, overall, no matter for a rear propulsive rotor or a front one, the aerodynamic drag of a helicopter at same forward flying speed will be almost same. Therefore, as the major contributor of the thrust of an ABC helicopter, the rear and front propulsive rotor will generate average thrust in close levels.

Furthermore, as shown in these figures, the vibration amplitude of thrust of the regular rear-installed propulsive rotor is larger than it of the nose-installed propulsive rotor. And the difference in the vibration amplitude of thrust is growing with the increasing of forward flying speed. It means, relative to a regular rear-installed propulsive rotor, the nose-installed propulsive rotor has an advantage in decreasing the vibration level of thrust for an ABC helicopter, and it is more obvious in higher advance ratios. This advantage for front propulsive rotor is mainly benefited from avoiding the direct aerodynamic impacts of the wake of main rotors.

On the other hand, Fig. 8(b) ~ Fig. 11(b) show the temporal variation in the power of the rear/front propulsive rotor over one revolution of main rotors at the advance ratio of 0.15, 0.2, 0.25 and 0.3. As shown in these figures, at a low advance ratio of 0.15, the power consumption of the nose-installed propulsive rotor is higher than it of the regular rear-installed propulsive rotor. When the advance ratio is set to be 0.2, the nose-installed propulsive rotor consumes slightly less power than the regular one. And with the further increasing of advance ratio, the nose-installed propulsive rotor is obviously more efficient. It means, relative to a regular rear-installed propulsive rotor, the nose-installed propulsive rotor has an advantage in decreasing the power consumption level for an ABC helicopter, and it is more obvious in higher advance ratios. The case will be the opposite, when the forward flying speed is getting very low.

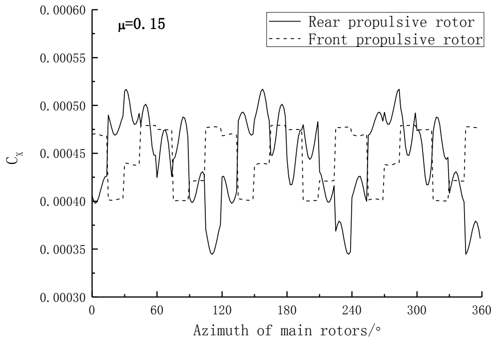

(a) Thrust coefficient

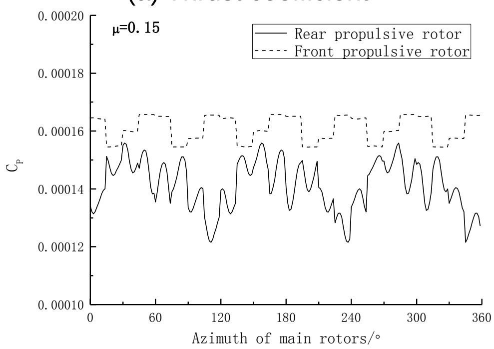

(b) Power coefficient

Fig. 8 Temporal variation in the thrust and power of the rear/front propulsive rotor over one revolution of main rotors（$\mu = 0.15$， $gZ = 0.56R$）

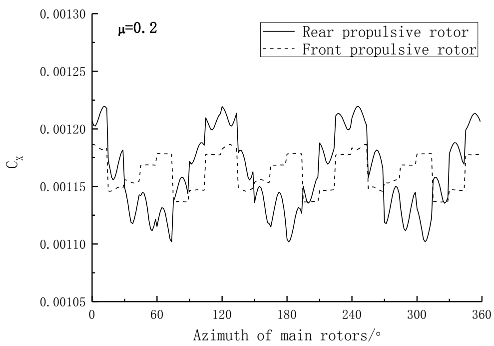

(a) Thrust coefficient

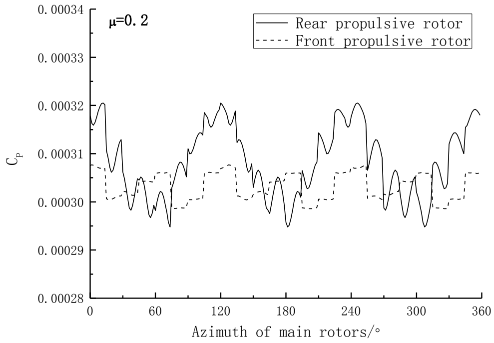

(b) Power coefficient

Fig. 9 Temporal variation in the thrust and power of the rear/front propulsive rotor over one revolution of main rotors（$\mu = 0.2$， $gZ = 0.56R$）

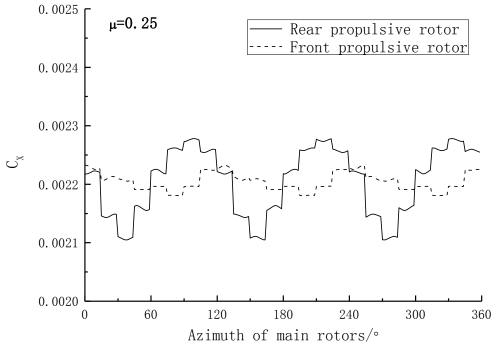

(a) Thrust coefficient

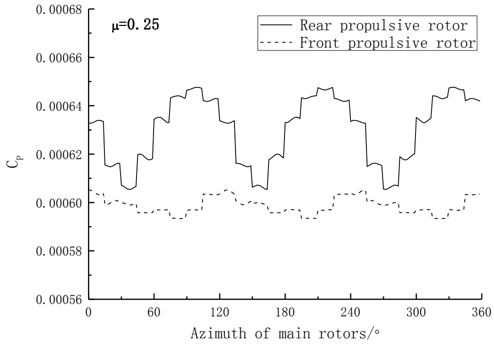

(b) Power coefficient

Fig. 10 Temporal variation in the thrust and power of the rear/front propulsive rotor over one revolution of main rotors（$\mu = 0.25$， $gZ = 0.56R$）

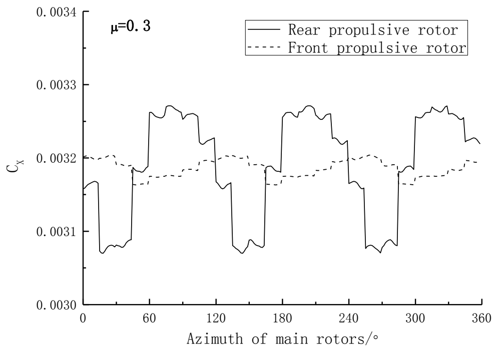

(a) Thrust coefficient

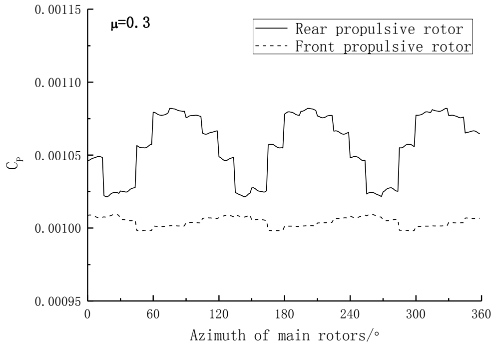

(b) Power coefficient

Fig. 11 Temporal variation in the thrust and power of the rear/front propulsive rotor over one revolution of main rotors（$\mu = 0.3$， $gZ = 0.56R$）

In addition, it should be noticed, for a regular rear-installed propulsive rotor, there are two types of vibration frequency existing in the temporal variation in the thrust and power of the propulsive rotor over one main rotor revolution at the same time at various advance ratios, i. e. one strong 3Ω component and another high-frequency 20Ω component. This situation may not be as same as it of the nose-installed propulsive rotor. For a front propulsive rotor, the two components of the vibration frequency are 6Ω and 20Ω at lower advance ratio as 0.15 and 0.2, as shown in Fig. 8 and 9. When the advance ratio is increased to 0.25 or 0.3, then the two components of the vibration frequency will develop into the 3Ω and 20Ω.

Furthermore, in order to understand the advantage of front propulsive rotor in power consumption in higher forward flying speed, distribution of inflow over the front propulsive rotor at various advance ratios is given in Fig. 10, where darker area represents larger values. As shown in the figure, there is significant difference between the front propulsive rotor and the regular rear propulsive rotor in the way of inflow distribution. For the nose-installed propulsive rotor, the upper half of the rotor disc is strongly interfered in aerodynamics by the blades of main rotors above it from a close distance, showing a distribution characteristic of asymmetrical center-diverging in inflow. And the inflow over lower half of the rotor disc is still presenting a distribution characteristic of horizontal-banding. It should be noticed, at all advance ratios, for the nose-installed propulsive rotor, the lower half of the rotor disc has the largest inflow speed, while the upper half of the rotor disc, being strongly interfered in aerodynamics by the blades of main rotors above it from a close distance, has the smallest inflow speed. In other words, the aerodynamic interference characteristics of the main rotors on the front propulsive rotor are decreasing its inflow. And with the decreasing in inflow on the propulsive rotor disc, the effective angle of attack of its blades will be increased. This means the aerodynamic performance of the propulsive rotor will be improved, when it is nose-installed under the main rotors. On the other hand, as discussed before, the direct aerodynamic impacts of the wake of main rotors on the regular rear propulsive rotor could raise the speed of inflow in the impacting zone on the propulsive rotor, as shown in Fig. 5. Then with the increasing in inflow on the propulsive rotor disc, the effective angle of attack of its blades will be decreased. This means the aerodynamic performance of the propulsive rotor will be degraded, when it is rear-installed in the wake of the main rotors. These aerodynamic characteristics will be more distinct in relative higher forward flying speed. In summary, the aerodynamic interference characteristics of the blades of main rotors on the front propulsive rotor, i. e. decreasing its inflow, is the main reason of that the nose-installed propulsive rotor acts obviously more efficient than the regular rear-installed propulsive rotor at relative higher advance ratios.

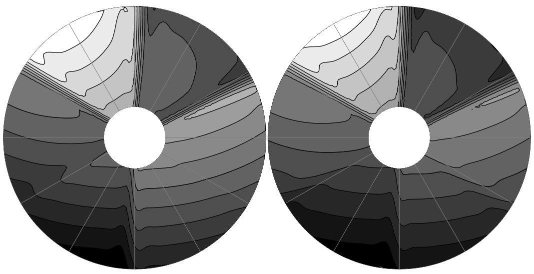

(a) $\mu = 0.15$ (b) $\mu = 0.2$

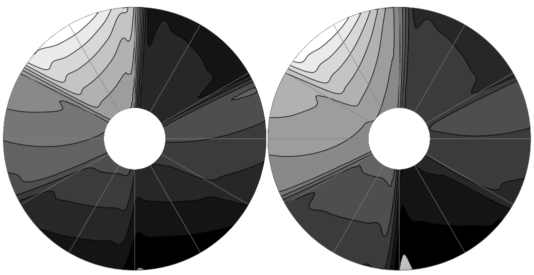

(c) $\mu = 0.25$ (d) $\mu = 0.3$

Fig. 12 Distribution of inflow over the front propulsive rotor at various advance ratios

In order to further investigate the aerodynamic interference characteristics of the main rotors on the front propulsive rotor, at the advance ratio of 0.3, the vertical spacing between the propeller hub of the propulsive rotor and the lower main rotor disc, i. e. gZ, is adjusted to more values such as closer distances $gZ = 0.31R$ and $gZ = 0.36R$, and a larger distance $gZ = 3.6R$. Then the new configurations of the ABC helicopter will be recalculated. It should be pointed out, in this research, the engineering feasibility is not much considered here, the helicopter configuration with a large distance of $gZ = 3.6R$ is just being calculated as a theoretical contrastive example with hardly any aerodynamic interference of the main rotors on the front propulsive rotor. Therefore Fig. 13 gives the temporal variation in the thrust and power of the rear/front propulsive rotor with various installation locations over one revolution of main rotors at the advance ratio of 0.3.

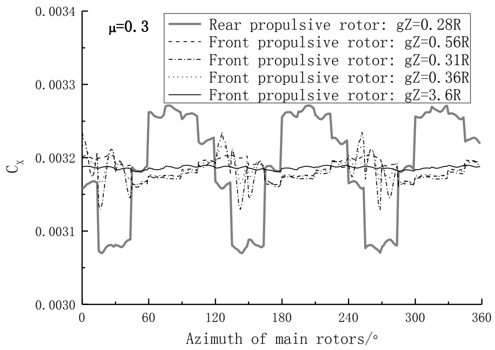

(a) Thrust coefficient

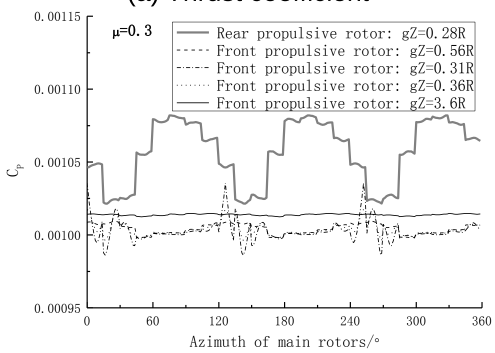

(b) Power coefficient

Fig. 13 Temporal variation in the thrust and power of the rear/front propulsive rotor with various installation locations over one revolution of main rotors ($\mu = 0.3$)

As shown in the Fig. 13(a), all the calculation examples present similar mean thrust over one revolution of main rotors. And for the closer vertical spacing between the propeller hub of the propulsive rotor and the lower main rotor disc, i. e. $gZ = 0.31R$ and $gZ = 0.36R$, the front propulsive rotor is clearly being more strongly interfered in aerodynamics by the blades of main rotors above it. At the azimuth of main rotors of 0°, 120° and 240°, there are acute oscillations in the temporal variation in the thrust of the front propulsive rotor. These azimuth angles indicate the times when the three blades of the lower main rotor are just passing over the front propulsive rotor. Moreover, for the helicopter configuration with closest vertical spacing of $gZ = 0.31R$, the oscillations in the temporal variation in the thrust of the front propulsive rotor at these azimuth angles are more acute than those of the other configurations, except ones of the regular configuration with rear propulsive rotor. And for the utmost vertical spacing of $gZ = 3.6R$, the oscillations in the thrust of the front propulsive rotor at these azimuth angles are the gentlest ones within all these calculation examples. It means, the nose-installed propulsive rotor will avoid the direct impact of the main rotor wakes, whereas it will still be interfered by the blades of main rotors in aerodynamics passing over it. And too close vertical spacing between the propeller hub of the propulsive rotor and the lower main rotor disc, will make acute oscillations in the temporal variation in the thrust of the front propulsive rotor, when the three blades of the lower main rotor are just passing over the front propulsive rotor.

On the other hand, as shown in the Fig. 13(b), at the azimuth of main rotors of 0°, 120° and 240°, there are acute oscillations in the temporal variation in the power of the front propulsive rotor, similar to the situation in thrust before. Specifically, regular rear propulsive rotor consumes more power than any configuration with the front propulsive rotor. Among all the configurations with the front propulsive rotor, the samples with $gZ = 0.31R$, $gZ = 0.36R$ and $gZ = 0.56R$ consume approximate power, while the sample with largest vertical spacing between the propeller hub of the propulsive rotor and the lower main rotor disc, i. e. $gZ = 3.6R$, is the least efficient one (still more efficient than the sample with the regular rear propulsive rotor). These results verify the analysis in this section before. In certain range of forward flying speed, the aerodynamic interference characteristics of the blades of main rotors on the front propulsive rotor, i. e. decreasing its inflow, will improve the aerodynamic performance and decrease the power consumption of the front propulsive rotor. This advantage will be weakened, if the vertical spacing between the propeller hub of the propulsive rotor and the lower main rotor disc is increased too much. On the other hand, the direct aerodynamic impacts of the wake of main rotors on the regular rear propulsive rotor, i. e. increasing its inflow, will degrade the aerodynamic performance and increase the power consumption of the regular rear propulsive rotor, as shown in Fig. 13(b).

4. CONCLUSIONS

In this research, based on the free-wake method, a comprehensive calculation model of an ABC rotor propeller-augmented compound helicopter has been established to investigate its interactional aerodynamic characteristics. And a new trim method for multi control solutions is presented. This research is focusing on the aerodynamic interference characteristics of the main rotors on the propulsive rotor and the effects of the installation location of propulsive rotor on its aerodynamic characteristics. And some new conclusions are drawn as follows.

(1) Relative to a regular rear-installed propulsive rotor, the nose-installed propulsive rotor has an advantage in decreasing the vibration level of thrust for an ABC helicopter, and it is more obvious in higher advance ratios. This advantage for front propulsive rotor is mainly benefited from avoiding the direct aerodynamic impacts of the wake of main rotors.

(2) In certain range of forward flying speed, the aerodynamic interference characteristics of the blades of main rotors on the front propulsive rotor, i. e. decreasing its inflow, will improve the aerodynamic performance and decrease the power consumption of the front propulsive rotor. This advantage will be weakened, if the vertical spacing between the propeller hub of the propulsive rotor and the lower main rotor disc is increased too much. On the other hand, the direct aerodynamic impacts of the wake of main rotors on the regular rear propulsive rotor, i. e. increasing its inflow, will degrade the aerodynamic performance and increase the power consumption of the regular rear propulsive rotor.

(3) There are two types of vibration frequency existing in the temporal variation in propulsive thrust and power over one main rotor revolution at the same time. One strong 3Ω component has a relatively longer wavelength, mainly caused by the wake of main rotors. And another component has a much higher frequency of about 20Ω, coming from the rotation of the propulsive rotor.

(4) Because of the effects of down wash flow of main rotors, the blades of propulsive rotor can be distinguished into two different operation conditions, i.e. the “climbing blade” and the “descending blade”. In the propulsive rotor disc, the “climbing blade” moves against the down wash flow of main rotors, therefore obtaining larger inflow velocity on the airfoil section and generating greater thrust. On the other hand, the “descending blade” moves along with the down wash flow of main rotors, therefore obtaining smaller inflow velocity on the airfoil section and generating less thrust. And larger forward flying speed will generate greater down wash flow of main rotors, which will aggravate the difference between “climbing/descending blades”.

REFERENCES

[1] Burgess R K. The ABC Rotor: a Historical Perspective. The 60th Annual Forum of the

American Helicopter Society, Baltimore, 2004.
[2] Robb R L. Hybrid Helicopters: Compounding the Quest for Speed. Vertiflite, 2006, 52 (2): 7-16.
[3] Orchard M, Newman S. The Fundamental Configuration and Design of the Compound Helicopter. Proceedings Of the Institution Of Mechanical Engineers Part G-Journal Of Aerospace Engineering, 2003, 217 (G6): 297-315.
[4] Quachenbush T R, Wachspress D A. Measurement and Analysis of High Advance Ratio Rotor Performance. The 64th Annual forum of the American Helicopter Society, Montreal, Canada, 2008.
[5] Bagai A, Leishman J G. Free-Wake Analysis of Tandem, Tilt-Rotor and Coaxial Rotor Configurations. Journal of the American Helicopter Society, 1996, 41 (3): 196-207.
[6] Lim J W, McAlister K W, Johnson W. Hover Performance Correlation for Full-Scale and Model-Scale Coaxial Rotors. Journal of the American Helicopter Society, 2009, 54 (3).
[7] Brown R E. Rotor Wake Modeling for Flight Dynamic Simulation of Helicopters. AIAA Journal, 2000, 38 (1): 57-63.
[8] Lakshminarayan V K, Baeder J D. High-Resolution Computational Investigation of Trimmed Coaxial Rotor Aerodynamics in Hover. Journal Of the American Helicopter Society, 2009, 54 (4).
[9] Kim H W, Kenyon A R, Duraisamy K, et al. Interactional Aerodynamics and Acoustics of a Propeller-Augmented Compound Coaxial Helicopter. The American Helicopter Society Specialists' Conference on Aeromechanics, San Francisco, CA, 2008.
[10] Brown R E, Line A J. Efficient High-Resolution Wake Modeling Using The Vorticity Transport Equation. AIAA Journal, 2005, 43 (7): 1434-1443.
[11] Zhao J G, He C J. A Viscous Vortex Particle Model for Rotor Wake and Interference Analysis. Journal of the American Helicopter Society, 2010, 55 (1).
[12] Kim H W, Brown R E. Impact of Trim Strategy and Rotor Stiffness on Coaxial Rotor Performance. The 1st AHS/KSASS International Forum on Rotorcraft Multidisciplinary Technology, Seoul, Korea, 2007.
[13] Kim H W, Kenyon A R, Brown R E, et al. Interactional Aerodynamics and Acoustics of a Hingeless Coaxial Helicopter with an Auxiliary Propeller in Forward Flight. Aeronautical Journal, 2009, 113 (1140): 65-78.
[14] Kim H W, Kenyon A R, Duraisamy K, et al. Interactional Aerodynamics and Acoustics of a Hingeless Coaxial Helicopter with an Auxiliary Propeller in Forward Flight. The International Powered Lift Conference, London, U. K., 2008.
[15] Cheney M C. The ABC Helicopter. Journal of the American Helicopter Society, 1969, 14 (4): 10-19.
[16] Burgess R K. Development of the ABC Rotor. The 27th Annual Forum of the American Helicopter Society, Washington, D. C., 1971.
[17] Leishman J G, Bhagwat M J, Bagai A. Free-Vortex Filament Methods for the Analysis of Helicopter Rotor Wakes. Journal of Aircraft, 2002, 39 (5): 759-775.
[18] Jain R, Conlisk A T. Interaction of Tip-Vortices in the Wake of a Two Bladed Rotor in Axial Flight. Journal of the American Helicopter Society, 2000, 45 (3): 157-164.